

# Highly reproducible high-index-contrast distributed Bragg reflectors with an oxidized digital-alloy AlGaAs

GUNWU JU<sup>a,b</sup>, SUBIN LEE<sup>c</sup>, BYUNG HOON NA<sup>d</sup>, HYUNG-JUN KIM<sup>b,e</sup>, YOUNG MIN SONG<sup>a,\*</sup>

<sup>a</sup>*School of Electrical Engineering and Computer Science, Gwangju Institute of Science and Technology (GIST), Gwangju 61005, Republic of Korea*

<sup>b</sup>*Center for Spintronics, Korea Institute of Science and Technology (KIST), Seoul 02792, South Korea*

<sup>c</sup>*Integrated Optics Laboratory, Advanced Photonics research Institute, Gwangju 61005, Republic of Korea*

<sup>d</sup>*Imaging Device Lab, Samsung Advanced Institute of Technology, Suwon-si, 16678, Republic of Korea*

<sup>e</sup>*Division of Nano & Information Technology, KIST School, Korea University of Science & Technology, Seoul 02792, South Korea*

We demonstrate uniform and reproducible high-index-contrast distributed Bragg reflectors (HIC-DBRs) by introducing an oxidized digital-alloy (DA) layer for low index materials. Fine-tunable DA- $\text{Al}_{0.98}\text{Ga}_{0.02}\text{As}$  layers, which consists of multiple stacks of 1 monolayer (ML)-thick GaAs and 49 ML-thick AlAs layers, are used for generating stable  $\text{Al}_x\text{O}_y$  layers instead of a conventional, bulk AlAs layers. Highly uniform arrays of oxidized alumina are obtained through a wet-oxidation of DA-AlGaAs layers, which enable practical use of HIC-DBRs for vertical cavity surface emitting lasers (VCSELs) and other resonant-cavity based optoelectronic devices. Detailed experiments together with optical calculations are also shown.

(Received September 25, 2017; accepted April 5, 2018)

**Keywords:** Digital-alloy, High-index-contrast, Distributed Bragg reflector, AlGaAs, Oxidation, VCSEL

## 1. Introduction

High-index-contrast (HIC) mirrors have been attracted much attention in optoelectronic applications such as wavelength filter [1], vertical cavity surface emitting lasers (VCSELs) [2, 3], resonant cavity enhanced photodetectors (RCEPDs) [4], and Si-integrated on-chip lasers [5]. Many fabrication techniques have been proposed to realize the HIC structure, such as wet-oxidation of Al-containing semiconductors [6], two dielectric materials [3], oblique angle deposition [7], and high-contrast grating (HCG) structures [8]. Fabrication of dielectric materials and HCG structures requires complicated and high-cost process. On the other hand, it is known that the formation of  $\text{Al}_x\text{O}_y$  layers as a low index material is relatively easier than other methods because of the simple wet-oxidation process. However, there are still critical issues on non-uniform oxidation characteristics of pure AlAs layer and poor mechanical strength at oxidized AlAs/GaAs interface, which prevent practical use of this concept [9]. In order to solve these problems, AlGaAs layers are inserted on both sides of the AlAs layer to improve oxide interface characteristics [10]. However, the oxidized AlGaAs layer shift the stopband and Fabry-Perot cavity wavelength.

It has been reported that reproducible fabrication is possible due to the highly selective oxidation characteristic of AlAs/GaAs digital-alloy (DA) [11]. Furthermore, binary material growth enhances thickness uniformity of the DBR, in which is more suited for uniform lasing of VCSEL [12]. In this study, oxidized DA-AlGaAs material is proposed that combines aforementioned two advantages

of growth and fabrication to produce a highly reproducible monolithic DBR. The wet oxidation is an essential fabrication process for forming aperture in conventional DBR VCSEL. Using this wet oxidation process, oxidized DA-DBR can be formed at the same time as aperture formation. The measured reflectivity results of oxidized DA-DBR show practical usability as a HIC-mirror and a good match to the simulated one.

## 2. Experimental details

Wet-oxidized pure AlAs/GaAs DBR and DA-AlGaAs/GaAs DBR were designed as shown in Fig. 1. The DA- $\text{Al}_{0.98}\text{Ga}_{0.02}\text{As}$  layer consists of 12 pairs of 1 monolayer (ML)-thick GaAs and 49 ML-thick AlAs layers. The thicknesses were designed for 980 nm center wavelength. The alumina oxide thickness was designed to be thicker than quarter wavelength thickness considering 12% shrinkage [6]. All structures were grown on (100) semi-insulating GaAs substrates by molecular beam epitaxy (MBE) system. The growth rate of GaAs and AlAs materials were measured by RHEED intensity oscillation before growth sequence. For lateral oxidation of the samples, 110  $\mu\text{m}$  diameter cylinder mesa patterns were etched by inductively coupled plasma reactive ion etching (ICP-RIE). The etched samples were immediately oxidized in a tube furnace at 420 °C under 2 l/min flow of nitrogen carrier which is bubbled through 90 °C deionized water reservoir. The oxidation was processed with different oxidation times to ascertain the oxidation rates.

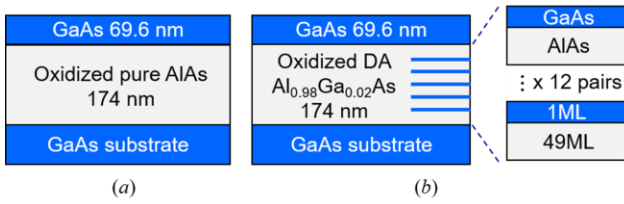


Fig. 1. Schematic cross-sectional view of designed (a) Pure AlAs/GaAs HIC-DBR structure and (b) DA-AlGaAs/GaAs HIC-DBR structure

### 3. Results and discussion

The oxidation region can be distinguished from unoxidized one because of different refractive index by means of an optical microscopy. The oxidation lengths are plotted in Fig. 2(a). An average oxidation rate of pure AlAs layer is 5.4 times faster than that of DA-AlGaAs

layer. This is because the thin GaAs layers embedded in DA have the effect of reducing the oxide channel thickness [13]. The rapid oxidation rate of the pure AlAs layer results in non-uniform oxidation characteristic. After 20 minute oxidation time, the pure AlAs shows non-uniform oxidation characteristics, while the DA-AlGaAs sample shows uniformly oxidized in spite of a relatively slow oxidation rate (Fig. 2(b)). This uniform oxidation characteristics are important in case of DA-DBR VCSEL since the multiple pairs of DA-AlGaAs should be uniformly oxidized. Dissimilar the normal DBR VCSEL, AlAs/GaAs digital-alloy can be used in aperture of monolithic VCSEL structures as well as DBRs. The oxidation rate of the DA-DBR layer is much faster than the aperture since the thickness of the DA-DBR layer is four times thicker than the aperture thickness [14]. Therefore, even if the diameters of the DA-DBR and aperture are the same, the DA-DBR is completely oxidized before the aperture closes.

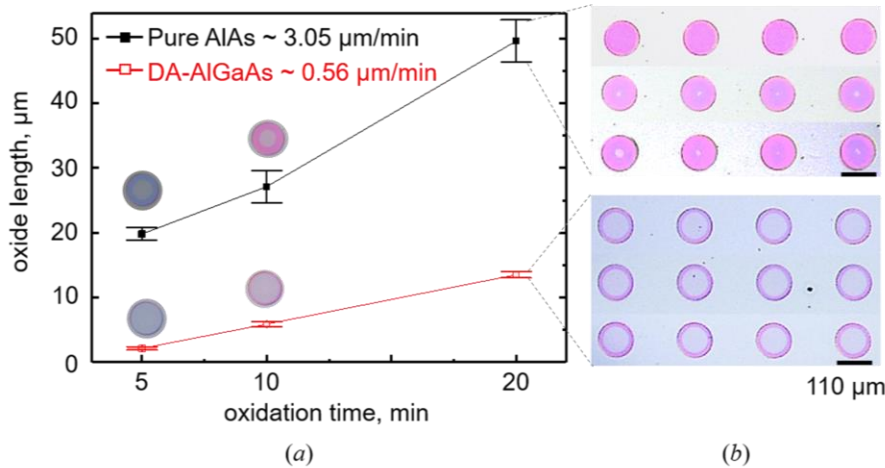


Fig. 2. Measured wet-oxidation results of (a) lateral oxidation length with different time and (b) top-view optical microscopic images of (up) pure AlAs (down) DA-AlGaAs mesas at 20 minute oxidation time

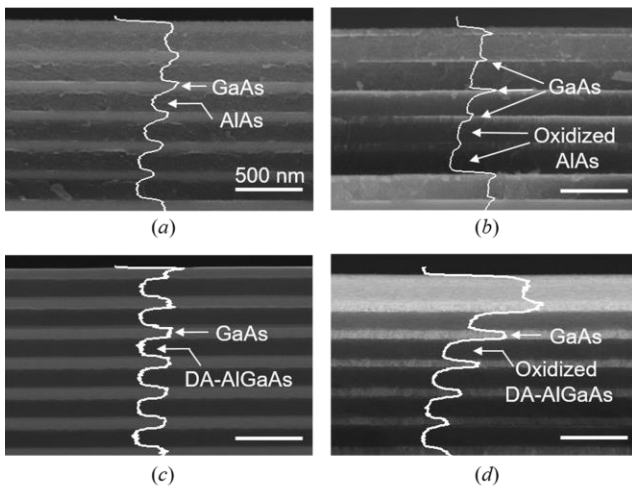


Fig. 3. Cross sectional SEM images of (a) as-grown pure AlAs/GaAs DBR, (b) oxidized pure AlAs/GaAs DBR, (c) as-grown DA-AlGaAs/GaAs DBR, and (d) oxidized DA-AlGaAs/GaAs DBR

Fig. 3 shows cross-sectional scanning electron microscopy (SEM) images of as-grown and wet-oxidized 6 pairs of DBR samples in which the white lines indicate the oxidation intensity profile. The DA-AlGaAs layer required an oxidation time of 100 minutes to completely oxidize. The interface between the pure AlAs and GaAs cannot be distinguished clearly after oxidation (Fig. 3(b)), but can be recognized before oxidation (Fig. 3(a)). This problem appears to be a blurred boundary due to the stress generated by using a pure AlAs [11]. The blurred interface cause poor reliability of DBR. On the other hand, the DA-AlGaAs sample shows clear interface both before (Fig. 3(c)) and after the wet-oxidation process (Fig. 3(d)). This result is caused by prevention of vertical reaction in the digital-alloy structure by thin GaAs layer [15]. In other words, ML-thick GaAs layers inserted retard the vertical oxidation in GaAs/AlAs digital-alloy structure because vertical oxidation rate of GaAs is much slower than AlAs. Consequently, it has been found that the stability of the

digital-alloy method is improved when it is used in the oxidation process.

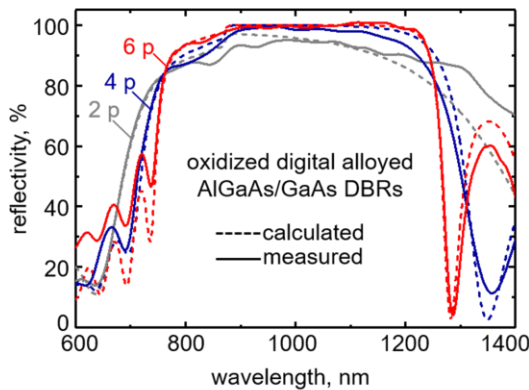


Fig. 4. Calculated and measured reflectivity spectra of oxidized DA-DBRs with the different pairs

The reflectivity of the oxidized DA-DBRs with different pairs was measured to evaluate the optical properties. The reflectivity was measured on the DBRs and an Au film of known reflectivity using an optical spectrum analyzer to obtain the absolute reflectivity. The measured reflectivity spectra show high reflectivity over a broad spectral wavelength range, which is almost similar to the calculated reflectivity (Fig. 4). As the number of DBR pairs increases, the center reflectance increases while maintaining a broad spectral bandwidth. It can be seen that even though the number of DBR pairs increases, the refractive index mismatch between each pair of DA-AlGaAs layer and GaAs layer is large. The center wavelength is  $\sim 1004$  nm, which is larger than designed wavelength. This is because the measured shrinkage is 7.3%, which is less than the previously reported shrinkage of 12% [6]. The 6 pairs of oxidized DA-DBR structures have a broad spectral bandwidth of 469 nm at reflectivity above 90%. This optical characteristic shows sufficient performance to be used as a mirror with high reliability in a resonant-cavity devices.

#### 4. Conclusions

The reliable monolithic HIC-DBR with oxidized DA-AlGaAs structure reveals the uniform oxidation characteristics and better mechanical stability than pure AlAs layer. The 6 pairs of oxidized DA-AlGaAs/GaAs DBR structure show the high reflectivity ( $> 90\%$ ) and wide bandwidth (469 nm). This highly reproducible

oxidized DA-DBR is expected to be a great contribution for monolithic resonant optoelectronic devices.

#### Acknowledgments

This work was supported by Institute for Information & communications Technology Promotion (IITP) grant funded by the Korea government (MSIP) (No.2017000709).

#### References

- [1] A. Liu, P. Wolf, J.-H. Schulze, D. Bimberg, *IEEE Photonics J.* **8**, 2700509 (2016).
- [2] M. H. MacDougal, G. M. Yang, A. E. Bond, C.-K. Lin, D. Tishinin, P. D. Dapkus, *IEEE Photonics Technol. Lett.* **8**, 310 (1996).
- [3] M. Muller, W. Hofmann, T. Grundl, M. Horn, P. Wolf, R. D. Nagel, M. C. Amann, *IEEE J. Sel. Top. Quantum Electron.* **17**, 1158 (2011).
- [4] S. Learkthanakhachon, A. Taghizadeh, G. C. Park, K. Yvind, I.-S. Chung, *Optics Express* **24**, 16512 (2016).
- [5] G. C. Park, W. Xue, M. Piels, D. Zibar, J. Mørk, E. Semenova, I.-S. Chung, *Sci. Rep.* **6**, 38801 (2016).
- [6] M. H. MacDougal, H. Zhao, P. D. Dapkus, M. Ziari, W. H. Steier, *Electron. Lett.* **30**, 1147 (1994).
- [7] S. J. Jang, Y. M. Song, C. I. Yeo, C. Y. Park, Y. T. Lee, *Opt. Mater. Express* **1**, 451 (2011).
- [8] C. J. Chang-Hasnain, Y. Zhou, M. C. Y. Huang, C. Chase, *IEEE J. Sel. Top. Quantum Electron.* **15**, 869 (2009).
- [9] T. Takamori, K. Takemasa, T. Kamijoh, *Appl. Phys. Lett.* **69**, 659 (1996).
- [10] M. H. MacDougal, P. D. Dapkus, *IEEE Photonics Technol. Lett.* **9**, 884 (1997).
- [11] G. W. Pickrell, J. H. Epple, K. L. Chang, K. C. Hsieh, K. Y. Cheng, *Appl. Phys. Lett.* **76**, 2544 (2000).
- [12] N. K. Cho, K. W. Kim, J. D. Song, W. J. Choi, J. I. Lee, *Solid State Commun.* **150**, 1955 (2010).
- [13] M. H. MacDougal, P. D. Dapkus, A. E. Bond, C.-K. Lin, J. Geske, *IEEE J. Sel. Top. Quantum Electron.* **3**, 905 (1997).
- [14] K. D. Choquette, K. M. Geib, C. I. Ashby, R. D. Twisten, O. Blum, H. Q. Hou, R. Hull, *IEEE J. Sel. Top. Quantum Electron.* **3**, 916 (1997).
- [15] I. Suárez, G. Almuneau, M. Condé, A. Arnoult, C. Fontaine, *J. Phys. D-Appl. Phys.* **42**, 175105 (2009).

\*Corresponding author: ymsong81@gmail.com